

Using DCFT for Multi-Target Detection in Distributed Radar Systems with Several Transmitters

Gokularam Muthukrishnan, S. Sruti, K. Giridhar
*TelWiSe Group, Department of Electrical Engineering,
 Indian Institute of Technology Madras,*

Chennai - 600036, India.

e-mail: {gokularam, srutisiva, k.giridhar}@telwise-research.com

Abstract—In distributed radar systems, when several transmitters radiate simultaneously, the reflected signals need to be distinguished at the receivers to detect various targets. If the transmit signals are in different frequency bands, they require a large overall bandwidth. Instead, a set of pseudo-orthogonal waveforms derived from the Zadoff-Chu (ZC) sequences could be accommodated in the same band, enabling the efficient use of available bandwidth for better range resolution. In such a design, special care must be given to the ‘near-far’ problem, where a reflection could possibly become difficult to detect due to the presence of stronger reflections. In this work, a scheme to detect multiple targets in such distributed radar systems is proposed. It performs successive cancellations (SC) starting from the strong, detectable reflections in the domain of the Discrete Chirp-Fourier Transform (DCFT) after compensating for Doppler shifts, enabling the subsequent detections of weaker targets which are not trivially detectable. Numerical simulations corroborate the efficacy and usefulness of the proposed method in detecting weak target reflections.

Index Terms—Distributed Radar, Multistatic Radar, Multi-Target Detection, Zadoff-Chu Sequences, Successive Cancellation, Discrete Chirp-Fourier Transform (DCFT).

I. INTRODUCTION

Distributed Radar Systems (DRS) [1]–[4], unlike conventional phased array-based monostatic radars, use multiple antennas at separate geographical locations for the transmission and reception of radio waves with the aim of detecting, localizing and tracking air-borne targets in the area of interest. When the transmitters and receivers are widely distributed such that the separations between them form a significant fraction of the target range, it is possible to collect the obliquely scattered energy from the targets at different aspect angles, and this spatial diversity can be exploited to improve the performance [5]. Observing radar cross-section (RCS) signatures of targets at different angles remarkably improves detection performance [6] and enhances target localization [7] and velocity estimation [8] accuracy. DRS also enables the detection of slow-moving targets and stealth targets and offers covertness and immunity to electronic counter-measures. It even facilitates imaging and classification of targets [9].

Two kinds of DRS exist: the passive and the active. Passive DRS operates with ‘illuminators of opportunity’ [10]; several types of transmitters of opportunity shall be used for the passive operation, e.g., DVB-T, DVB-S, DAB, FM, communication links or even existing monostatic radars. However,

such systems exploit waveforms that are not necessarily good for target detection, resulting in poor performance despite the complex signal processing at the receivers. In this paper, we focus on an active, continuous wave (CW) DRS, which employs several dedicated transmitters that continuously radiate repetitions of a specific wave pattern that are known to the receivers. These waveforms are reflected back from the prospective targets toward the receive antennas, which can then be processed and fused at various levels.

A received waveform after impinging a target would be delayed, attenuated and also shifted in frequency if the target is in motion. The time delay (TD) and Doppler shift (DS) are the key signatures that a target leaves in a waveform. TD corresponds to the total distance travelled by the waveform (bistatic range, BR), whose rate of change (bistatic range rate, BRR) translates to DS in the waveform. Once a target is detected, estimated TDs and DSs of the reflected waveforms at various receivers shall be fused to estimate its kinematic state, i.e., position and velocity [8]. At the *matched filter* receivers that operate non-coherently, targets are first detected, and the corresponding TD and DS are then estimated by computing the cross ambiguity function between received and reference transmit signals.

For good performance, waveforms must have tolerance to Doppler and low autocorrelation side lobes. Also, it is desirable to have a low Peak to Average Power Ratio (PAPR) for efficient transmission. The use of periodic modulated CW signals can yield perfect autocorrelation [11], and several spreading codes have been studied in the literature for this purpose [12], [13]. Constant Amplitude Zero Auto-Correlation (CAZAC) sequences exhibit ideal time localization and transmission efficiency. Certain classes of CAZAC sequences have been used in radars for years. Among the CAZAC sequences, Zadoff-Chu (ZC) [14] polyphase codes are a good choice here because of their flexible length and robustness against Doppler effects [12]. ZC sequences are *perfect sequences* with an ideal periodic autocorrelation function (PACF) and have unit PAPR. Periodic cross-correlation function (PCCF) between two ZC codes from different seeds is also low and documented in [15].

The use of multiple transmitters offers robust, fault-resilient functioning of DRS even if some transmitters are compromised. Also, having more transmitters improves the coverage and provides better localization accuracy [16]. However, it has its own set of challenges; when the receiver collects echoes

from multiple transmitters, they have to be uniquely identified and separately processed to leverage the benefits. Thus, mutual interference between the different transmit signals should be minimized. Transmitters can operate orthogonally in frequency with no bandwidth overlap or in time without simultaneous radiations. The accuracy of TD measurements is limited by the bandwidth, and hence, the accuracy of the target position estimates depends strongly on the bandwidth [7]. The paucity of available spectrum renders the sharing of available bandwidth among the transmitters difficult without compromising localization accuracy. Longer integration times are required for good Doppler resolution. Also, longer signal duration results in better accuracy of the target speed estimation [17]; consequently, switching between the available transmitters before the targets have significantly moved would result in poor performance.

By leaving these options, waveforms are necessitated to be mutually orthogonal under correlation (i.e., orthogonal in code) while transmitted simultaneously over the same spectrum. A set of waveforms with an impulsive autocorrelation function and zero mutual cross-correlation functions is desirable. However, it is impossible to design such an ideal set of sequences [18], [19]. However, to the rescue, polyphase codes, such as the ZC codes, have good cross-correlation properties alongside ideal PACF [20]. Prime length ZC codes attain the tightest possible suppression by a factor of \sqrt{N} for perfect sequences, where N is the code length; for other cases, there is only a graceful degradation [15]. For these reasons, we consider ZC sequences for the active CW DRS with several transmitters.

When there are several targets in the observed space, each one of them needs to be detected, localized and tracked separately. However, when the targets are at different heights, the power of the echoed transmit waveforms will have large variations, and some targets might go undetected even with good PCCF. Reflections from targets which are high or which have low RCS will be weak; correlation side lobes arising from the strong reflections from certain targets might mask such weak target echoes, rendering them undetectable and, consequently, limiting the range of observable space. Thus, appropriate processing techniques to detect need to be designed such that weak reflections from targets can be identified when there are strong reflections from other targets. In this work, we address this problem.

A. Motivation

Several signal processing techniques in DRS draw inspiration from those in MIMO wireless communication systems [2] and one such idea, namely the successive cancellation (SC) [21], [22], is used in this work for multi-target detection in active CW DRS with several transmitters. It can be observed that ZC sequences resemble samples of linear frequency modulated (LFM) waveforms (or chirps) used in conventional radars, and the seed of a sequence determines the sweep rate of the frequency. Discrete Chirp-Fourier Transform (DCFT) [23] is a generalization of Discrete Fourier Transform (DFT) [24] that can reveal the presence of chirps when a variable

in the transform is matched to the sweep rate. Consequently, a ZC sequence present in the received composite signal can be transformed to an impulse in the transform domain by matching the chirp rate variable to the seed of the sequence, where it can be filtered by nulling the impulse. Since this transform is invertible, the ZC sequence would have been excised in the time domain after this step, leaving room to detect any weaker ZC sequence present in the residue. By appropriately handling the Doppler in the reflected waveforms, this process can be repeated until no more detectable target reflections are present in the residue. This idea for multi-target detection is formally presented in Section III.

B. Basic Notations

In this article, j indicates the imaginary unit, i.e., $j = \sqrt{-1}$. The set of all complex numbers, the set of all integers, and the set of all positive integers are denoted as \mathbb{C} , \mathbb{Z} and \mathbb{N} , respectively. The complex conjugate of $v \in \mathbb{C}$ is written as v^* . $\text{gcd}(a, b)$ is the greatest common divisor of $a \in \mathbb{Z}$ and $b \in \mathbb{Z}$ and is non-negative by convention; if $\text{gcd}(a, b) = 1$, a and b are said to be relatively prime, and $\text{gcd}(a, 0) = |a|$. The modulo operator $\langle a \rangle_b$ provides the (non-negative) remainder of the Euclidean division of $a \in \mathbb{Z}$ by $b \in \mathbb{Z} \setminus \{0\}$; hence, $\langle a \rangle_b \in \{0, 1, \dots, |b| - 1\}$.

The Kronecker delta function is denoted as $\delta[\cdot]$. Consider two complex-valued N -length sequences, $x[n]$ and $y[n]$, $n = 0, 1, \dots, N - 1$. The periodic correlation function between them at the shift $l \in \{0, 1, \dots, N - 1\}$ is evaluated as $(x \otimes y)[l] = \sum_{n=0}^{N-1} x[n]y^*[\langle n - l \rangle_N]$; if both the sequences are the same, it is called periodic autocorrelation function (PACF), else periodic cross-correlation function (PCCF).

II. BACKGROUND AND SYSTEM MODEL

Let us take a short digression to review the necessary background and introduce the system model.

A. Zadoff-Chu Sequences

Zadoff-Chu (ZC) sequences [14] are complex-valued codes that are widely used in various signal processing applications [25]–[27]. They are constant amplitude, polyphase sequences whose elements are roots of unity.

Definition 1. The ZC sequence of length N is given by

$$z_{u,N}[n] = W_N^{un(n+\langle N \rangle_2)/2}, \quad n = 0, 1, \dots, N - 1, \quad (1)$$

where $W_N = e^{-j2\pi/N}$ denotes the well-known *twiddle factor*, and $u \in \mathbb{Z}$, known as the *seed* of the sequence, is relatively prime to N .

Thus, the seed- u ZC sequence is a unique code comprising a particular arrangement of N -th roots of unity arising from the choice of primitive root W_N^u .

ZC sequences have several nice properties. It can be observed that any ZC sequence is periodic with period N , i.e., $z_{u,N}[n] = z_{u,N}[\langle n \rangle_N] \quad \forall n \in \mathbb{Z}$; thus, Definition 1 holds for all $n \in \mathbb{Z}$. Also, a time delay in a ZC sequence manifests as a Doppler shift to the original waveform, i.e.,

$z_{u,N}[n-l] = z_{u,N}[n] \times z_{u,N}[-l] W_N^{-uln}$; thus, ZC sequences exhibit time-frequency coupling.

The DFT or IDFT of a ZC Sequence is again a ZC Sequence [28]. Also, ZC sequences have desirable correlation characteristics, which are listed below, making them well-suited for radar and communication applications.

- (i) ZC sequences are perfect sequences, and they are orthogonal to cyclically shifted copies of themselves, irrespective of the seed [14]. Thus, they have an ideal PACF of $N\delta[\langle l \rangle_N]$.
- (ii) The maximum absolute value of the PCCF between the length- N ZC sequences arising from two different seeds, a and b , is given by $\sqrt{\tau N}$, where $\tau = \gcd(N, a - b)$ [15].

Variations such as cyclic shifts, the addition of a constant phase, or conjugating the entire code will not affect the PACF characteristics of the ZC sequences.

ZC codes can be interpreted as discrete counterparts of linear frequency modulated (LFM) signals (or chirps); the sweep rate of the frequency is determined by the seed of the ZC sequence. Subsequently, their energies are concentrated as (aliased) *lines* in the time-frequency plane, as observed in the normalized spectrogram of a ZC sequence in Figure 1. This interpretation makes the use of signal processing tools available for chirps to ZC sequences possible: we witness one such instance in the sequel through DCFT.

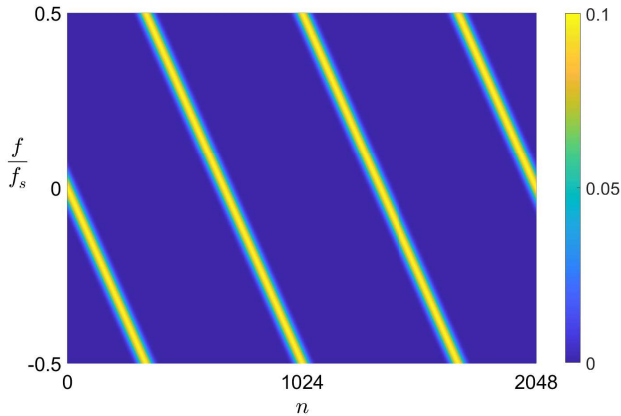


Fig. 1. Normalized spectrogram of Zadoff-Chu sequence of length $N = 2048$ with seed $u = 3$.

B. Discrete Chirp-Fourier Transform

Following the observation that the ZC sequences are the sampled chirp signals, we now introduce a tool for filtering them in the receivers. Classical Fourier spectrum analysis tools like DFT become useless for chirps as they cannot be used to analyze wideband and non-stationary signals. The Discrete Chirp-Fourier Transform (DCFT) [23] generalizes the DFT to facilitate the analysis of chirp-type signals, and it comes in handy in radar applications. DCFT has been used for detection [29] and parameter estimation [30] of multi-component chirp signals, Detection for high-speed manoeuvring targets [31] and

identification of jamming [32].

DCFT is parametrized by the chirp rate variable β and the frequency index k . DCFT is related to Fractional Fourier Transform (FrFT) [33], and the variable β in the DCFT corresponds to the rotation angle in FrFT. DCFT and its inverse are defined as follows¹.

Definition 2 (DCFT and IDCFT). The N -point DCFT of an N -length sequence $x[n]$, $n = 0, 1, \dots, N - 1$ is given by

$$X_c[k, \beta] = \frac{1}{\sqrt{N}} \sum_{n=0}^{N-1} x[n] W_N^{kn - \beta n^2/2}, \quad (2)$$

$$k = 0, 1, \dots, N - 1, \quad \beta = 0, 1, \dots, \lceil \frac{N}{2} \rceil - 2.$$

Thus, $\{X_c[k, \beta]\}_{k=0}^{N-1}$ is the DFT of $x[n] W_N^{-\beta n^2/2}$ for an arbitrarily fixed $\beta \in \{0, 1, \dots, \lceil \frac{N}{2} \rceil - 2\}$, and the inverse DCFT (IDCFT) can be defined as

$$x[n] = \frac{1}{\sqrt{N}} \sum_{k=0}^{N-1} X_c[k, \beta] W_N^{-kn + \beta n^2/2}, \quad n = 0, 1, \dots, N - 1. \quad (3)$$

Thus, the DCFT reduces to the DFT when $\beta = 0$.

Remark 1. For the remainder of this paper, we will consider only even length ZC sequences N , $N \in 2\mathbb{N}$, particularly N , which is a power of 2. This is mainly to facilitate the implementation of DCFT and PCCF via the Fast Fourier Transform (FFT) algorithm with lesser computations. In such cases, any odd integer u will be relatively prime to N . The seed u is further restricted to be in the set $u \in \{1, 2, \dots, N/2 - 2\}$ in order to unambiguously match β and u .

C. System Model

Let us consider an active CW DRS comprising of M widely separated transmit antennas, each of which periodically emits an N -length ZC waveform of unique seed, and the reflections of these waveforms from the K targets present in the observation area are collected by L receive antennas, themselves widely placed. The samples of the transmit signal are given by

$$s_i[n] = z_{u_i, N}[n], \quad i = 1, 2, \dots, M, \quad (4)$$

where $u_i \in \{1, \dots, N/2 - 2\}$, $u_i \neq u_m$ for $i \neq m$ and $\gcd(u_i, N) = 1 \quad \forall i \in 1, 2, \dots, M$. Optimal selection of ZC codes for transmitters meeting these constraints can be done by picking seeds based on the results presented in [15]. However, our numerical studies indicated that these choices did not impact the performance much, and therefore, we simply picked the first M odd integers as seeds, i.e., $u_i = 2i - 1, \quad i = 1, 2, \dots, M$.

In this work, we assume that all the L targets are point targets, occupying a single range-Doppler bin at the receivers' matched filters at most. Also, the targets are assumed to move approximately at constant velocities over the coherence interval. It is assumed that there is no line of sight between the transmitters and the receivers, and the direct signal from any

¹We consider the modified DCFT, MDCFT I in [34], with a slight change.

transmitter is not observed by the receivers through the use of appropriate antenna beam patterns. We also assume that there is no clutter since the targets are air-borne.

Each receiver collects the signals reflected by the targets. The samples of the received baseband signals are modelled as

$$v_p[n] = v_p^{(0)}[n] + \gamma_p[n], \quad p = 1, 2, \dots, L, \quad \text{where}$$

$$v_p^{(0)}[n] = \sum_{i=1}^M \sum_{q=1}^K \alpha_{ip}^{(q)} s_i[n - l_{ip}^{(q)}] \exp(j2\pi\xi_{ip}^{(q)} n), \quad (5)$$

and $\gamma_p[n]$ is additive white Gaussian noise. Here, $\alpha_{ip}^{(q)}$, $l_{ip}^{(q)}$ and $\xi_{ip}^{(q)}$ are, respectively, the unknown (complex) amplitude, the time delay and the (normalized) Doppler shift encountered by the i -th transmit waveform collected by the p -th receiver after reflection at the q -th target. With respect to noise, the target echo signals are boosted by the processing gain resulting from the correlation. The targets are detected, and TD and DS are estimated through range-Doppler correlation; each receiver contains M correlation filters, each corresponding to a transmit sequence. The received signal over ηN samples, where $\eta \in \mathbb{N}$, is cross-correlated with the frequency-shifted η replicas of transmit sequences (where the frequency shifts correspond to hypothesized values for the Doppler in the received signal) to produce the range-Doppler map for a coherent integration interval; over each such map, target detections are performed.

III. SC ALGORITHM USING DCFT

When the received signal is composed of reflected echoes of various transmit signals, the targets resulting in weak reflections cannot be detected when the cross-correlation side lobes corresponding to stronger target reflections are larger than the compression gain from autocorrelation of the weaker reflection. This scenario occurs often in practice when a target has relatively low RCS or when the target is very far from the transmitter and receiver relative to some other target yet within the coverage area. We propose a solution to address this problem in multi-transmitter DRS using ZC sequences.

For an even-length, time-delayed ZC sequence $z_{u,N}[n - l]$, $N \in 2\mathbb{N}$, it can be seen that when the chirp rate β is matched to the seed of the sequence, i.e., $\beta = u$, the DCFT is reduced to the DFT and the DCFT results in a peak of magnitude \sqrt{N} at $k = \langle ul \rangle_N$. The magnitude of DCFT under the unmatched case is bounded by a value, which will be gracefully larger than 1, and this shall be proven by observing the relation between ZC sequences' PACFs and PCCFs and their DCFTs and proceeding similarly to [15]. By utilizing this property, a new algorithm to detect multiple targets based on successive cancellations in the DCFT domain is proposed.

A reflection of a ZC sequence present in the composite received signal will get transformed into an impulse in the DCFT domain when β is matched to the seed of the sequence. We propose nulling such impulses to remove the interference; once the inverse transform is applied, the corresponding ZC sequence would have been removed in the time domain. After such a cancellation, any other weaker reflection present in the residue might be visible, as removing the stronger ZC sequence also removes the corresponding side lobes in the

Algorithm 1 Multi-Target Detection via Successive Cancellation in the DCFT Domain - SC-DCFT.

Input: Received signal at the p -th receiver $v_p[n]$.

Initialization: Initialize the residual signal, $r_p[n] = v_p[n]$.

```

1: repeat
2:   for  $i = 1, 2, \dots, M$  do
3:     Compute the range-Doppler map through
       ambiguity function between  $r_p[n]$  and  $s_i[n]$ .
4:     for each detection  $\kappa$  in the range-Doppler map, do
5:       Estimate the delay  $l_{ip}^{(\kappa)}$  and Doppler shift  $\xi_{ip}^{(\kappa)}$ .
6:        $g_p[k] = \text{DCFT}_{\beta=u_i} \left\{ r_p[n] \exp(-j2\pi\xi_{ip}^{(\kappa)}) \right\}$ .
7:        $g_p[\langle ul_{ip}^{(\kappa)} \rangle_N] \leftarrow 0$ .
8:        $r_p[n] \leftarrow \text{IDCFT}_{\beta=u_i} \{ g_p[k] \} \times \exp(j2\pi\xi_{ip}^{(\kappa)})$ .
9:     end for
10:  end for
11: until no further targets are detected.

```

Output: Detected targets and their TD and DS measurements.

subsequent range-Doppler maps. This renders the detection of targets which result in weak reflections possible. By successively performing such cancellations in the DCFT domain, more targets which were originally undetectable can now be detected. This process can be repeated until no more detectable target reflections are in the residue.

However, in the presence of Doppler, ideal behaviour is gradually lost, and a ZC sequence will not get transformed into an impulse by the DCFT but rather into a Dirichlet (periodic) sinc (see [35, eq. (17)]). Also, the increase in Doppler shift results in a rapid decrease of the peak. This presents a challenge, and the SC has to be performed after appropriate handling of the Doppler. Since the Doppler of the detected target can be estimated from the range-Doppler map, the entire signal can be de-rotated in order to minimize the Doppler present in the strong reflection from a detected target. Under the DCFT, such a strong replica of the ZC sequence with a low residual Doppler would become an impulse and can be filtered. After performing this step, the residues can be rotated back to remove the Doppler, which was injected into the weaker reflections when de-rotating the strong reflections. By proceeding this way, the targets resulting in weaker echoes can be detected through SC.

The proposed scheme is summarized in Algorithm 1.

IV. SIMULATION RESULTS

Computer simulations are performed to validate the proposed solution. We consider a VHF DRS operating on a 20MHz band centered at 500MHz. The system employs several CW transmitters which transmit ZC sequences of length $N = 2048$, resulting in a pulse duration of $102.4\mu\text{s}$; coherent integration of received waveform is performed over $\eta = 8$ pulses, resulting in a coherent integration time of $819.2\mu\text{s}$. We mostly consider the system configuration presented in Figure 2, where positions are marked in metres and velocities are

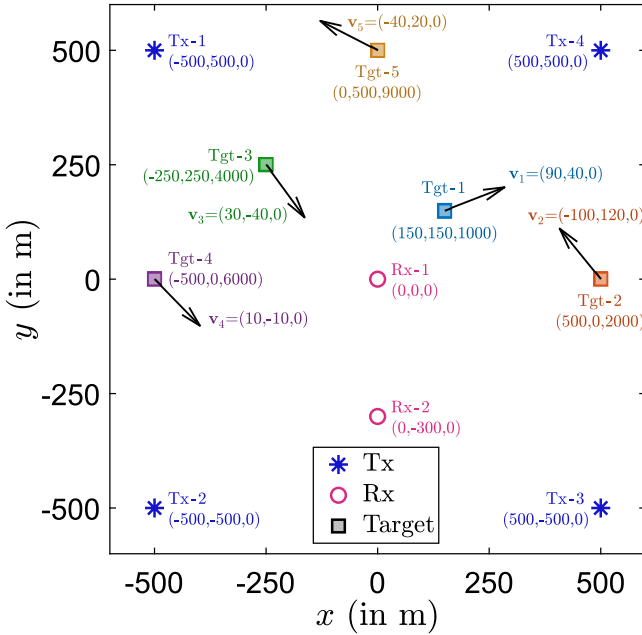


Fig. 2. Top view of the system geometry of the simulated DRS.

marked in m/s. There are four transmitters (Tx-1:Tx-4) and two receivers (Rx-1 and Rx-2), which are ground-based and stationary. All the transmitters radiate with the same power of 500W. There are five air-borne targets (Tgt-1:Tgt-5) that are moving with constant velocities (labelled as $\mathbf{v}_1:\mathbf{v}_5$). All the targets in the figure have unit RCS. The delays, Doppler shifts and attenuations of the received waveforms in (5) are accordingly determined from this system configuration. The performance is studied under four different cases.

- **Case 1:** All four transmitters are radiating, and all five targets are in the surveillance area.
- **Case 2:** All the targets are in the surveillance area, but only two transmitters (Tx-1 and Tx-3) radiate.
- **Case 3:** All the transmitters are radiating, but only two targets (Tgt-2 and Tgt-4) are present in the area.
- **Case 4:** All the transmitters are radiating, and two targets (Tgt-3 and Tgt-6) are present. Tgt-6 (not marked in the figure, located at $(-500, 0, 3975)$, $\mathbf{v}_6 = \mathbf{v}_4$) has an altitude very close to that of Tgt-3 and has a low RCS of 0.025m^2 , 16dB below that of Tgt-3, and results in colliding peaks in two of the four matched filters in Rx-1.

We study the detection rate (i.e., the fraction of times a target gets correctly) as a function of composite Signal-to-Noise-Ratio (SNR) at the receivers, which is the ratio of powers of composite received signal, $v_p^{(0)}[n]$, and the noise, $\gamma_p[n]$, in (5) and consider 2000 Monte-Carlo trials. The detection rates of each target in each of the transmit waveforms are individually shown, and the rates corresponding to detection in at least one waveform and all the waveforms are also studied.

Results corresponding to Case 1 are presented in Figure 3 and Table I. Figures 3a and 3b show the detection rates of the proposed approach (SC-DCFT in Algorithm 1) and those of raw detection in Rx-1. The corresponding results for

Rx-2 are provided in Figures 3c and 3d. From the plots, it is evident that in both the receivers, the raw detection can detect only two low-flying targets (Tgt-1 and Tgt-6) in all the transmit waveforms; additionally, in Rx-2, Tgt-3 at the altitude of 4km gets detected in the waveform of Tx-4. Meanwhile, the proposed scheme results in the *detection of all the targets in all the transmit waveforms*. In addition, the detection rates for Tgt-2 are significantly better than the raw detection; SC-DCFT detects Tgt-2 in all the transmit waveforms at the composite SNR of -7dB , which is not the case with raw detection. The raw detection method could not detect since its performance is heavily limited by interference due to reflections from Tgt-1 and Tgt-2. The performance of the proposed scheme is mainly *limited by noise*, and the detections of Tgt-3:Tgt-5 occur at high composite SNRs just because of the weak contributions of corresponding reflections to the composite signal $v_p^{(0)}[n]$.

In Table I, the detection performance of our scheme is compared with that of the conventional successive cancellation in the time domain, where the time domain replicas of the detected waveforms are reconstructed from estimated amplitude, delay and Doppler estimates from the range-Doppler map (as in (5)), and subtracted from the received signal to further detect other targets from the residue. We study the detection rates of the highest target, Tgt-5, in the waveform of TX-3 in Rx-1. Though SC in the time domain, unlike the raw detection, can detect Tgt-5, the proposed scheme outperforms it with better detection rates. These results show the efficacy of the proposed method in handling multiple targets by properly handling interferences from strong reflections, limiting the performance only to the noise level.

TABLE I
DETECTION RATES OF TARGET-5 IN CASE 1 WITH RESPECT TO THE THIRD TRANSMITTER IN THE FIRST RECEIVER

Composite SNR (dB)	9	10	11	12	13	14
Proposed SC-DCFT	0.0370	0.0835	0.1745	0.3305	0.5030	0.7050
SC in Time Domain	0.0040	0.0195	0.0650	0.1810	0.3995	0.6680

In Figure 4, the detection performance in Rx-1 is presented for the case with a lesser number of transmitters than before (Case 2), and in Figure 5, it is plotted for a scenario with a lesser number of transmitters (Case 3). Both cases offer lesser overall interference than before. Despite that, raw detection could not detect any targets which were undetected in the previous study. The proposed approach is powerful and detects all the targets in all the waveforms, and it also offers performance improvement in these cases where the interference is less, which is evident by comparing Figures 4a and 5a with Figure 3a. For the challenging Case 4, the results are plotted in Figure 6. It can be observed again that the proposed method offers better performance than the raw detector, particularly for the detection of Tgt-6.

Finally, in Figure 7, we study the performance of the proposed method for the case when waveforms are band-limited to 90% of the available band. In this scenario, the transmit

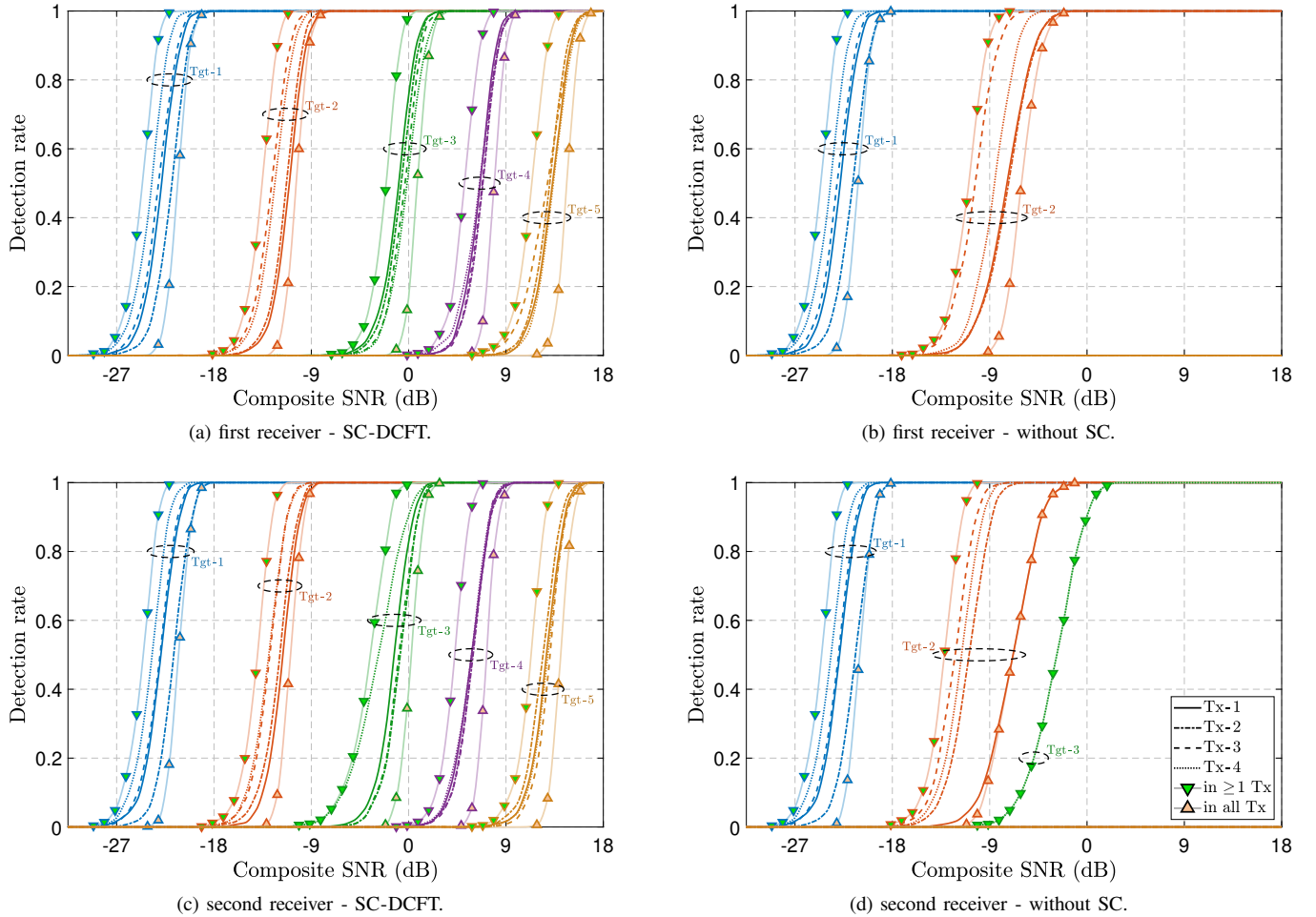


Fig. 3. Detection rates of the targets for Case 1.

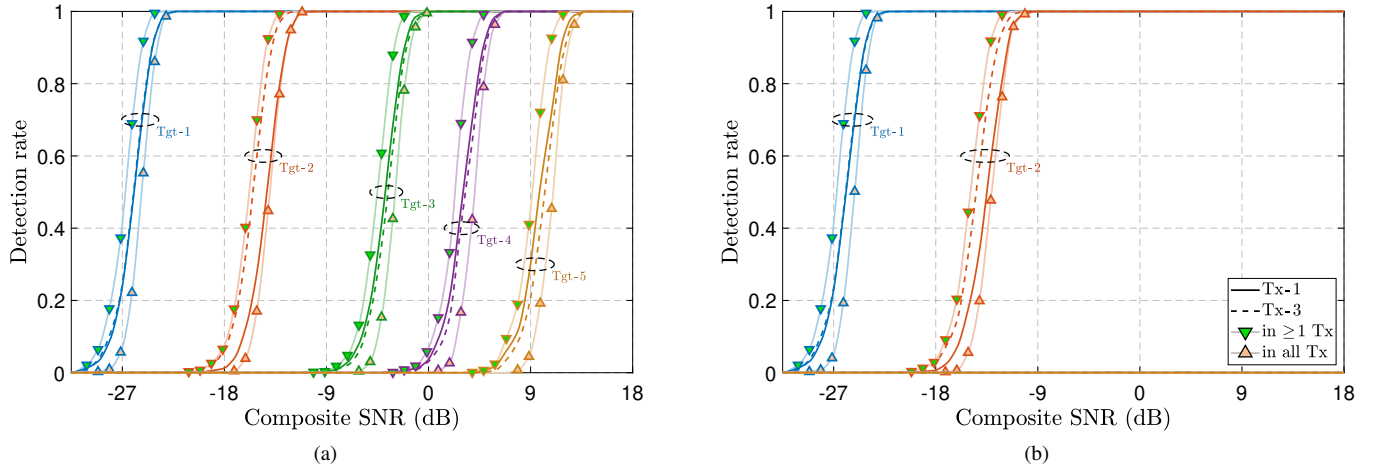


Fig. 4. Detection rates of the targets in Rx-1 for Case 2, (a) SC-DCFT (b) without SC.

signals will not be a perfect ZC sequence; hence, performance deterioration is expected. However, the performance is still good, detecting up to four targets. Future work shall focus on improving the performance further in such practical settings.

V. CONCLUSIONS

In this work, we have described a novel multi-target detection scheme based on successive cancellations for continuous wave, distributed radar systems functioning with several transmitters that radiate Zadoff-Chu sequences in the same band. In the receivers, successive cancellations are performed using the

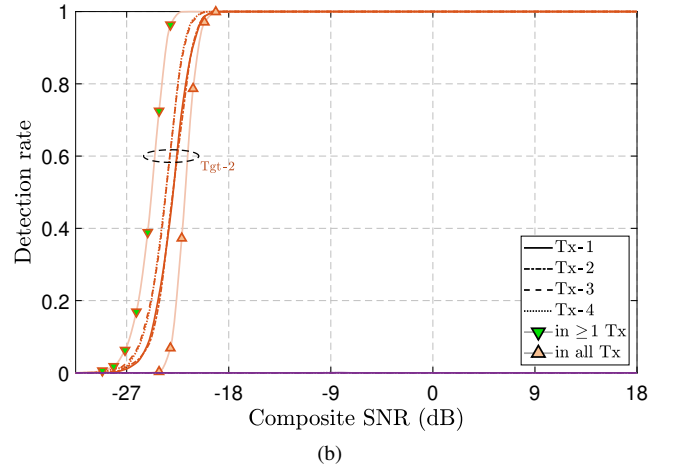
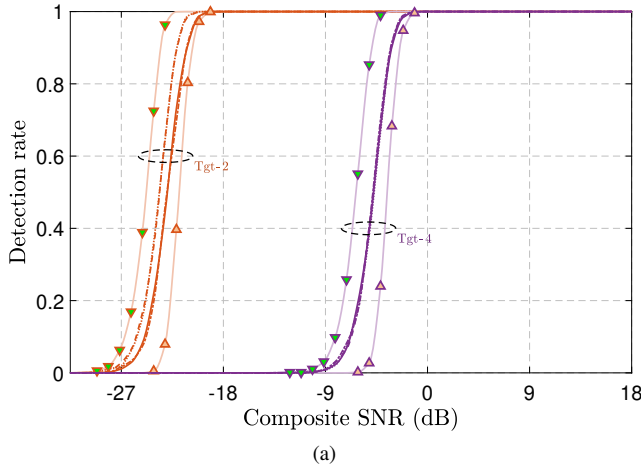


Fig. 5. Detection rates of the targets in Rx-1 for Case 3, (a) SC-DCFT (b) without SC.

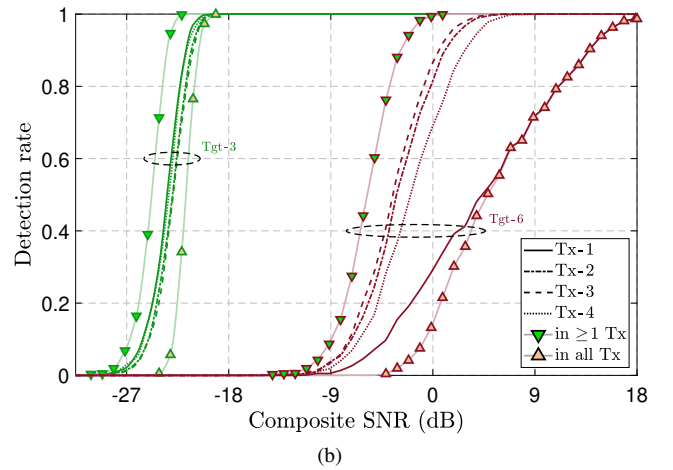
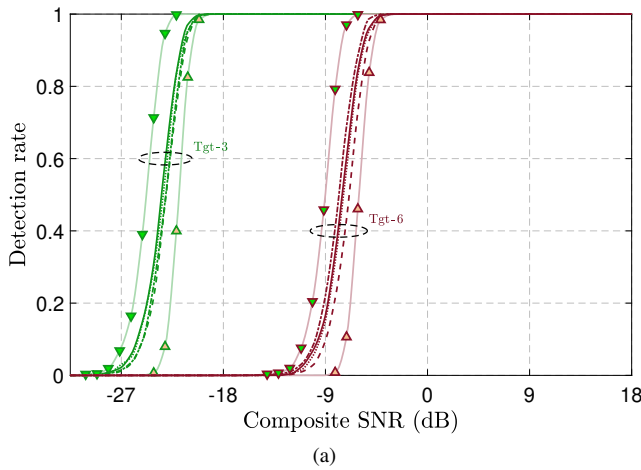


Fig. 6. Detection rates of the targets in Rx-1 for Case 4, (a) SC-DCFT (b) without SC

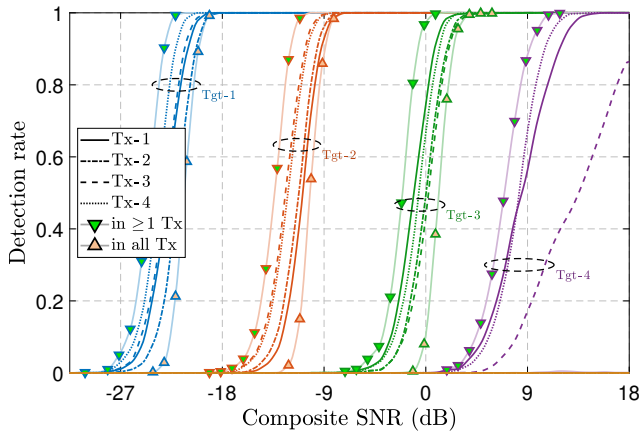


Fig. 7. Detection rates of the targets under band limited waveforms in Rx-1 for Case 1 .

Discrete Chirp-Fourier Transform after carefully compensating for the Doppler shifts. This minimizes the interference to other weak target reflections in the received signal, which get detected subsequently. Through extensive numerical simulations,

the effectiveness of the proposed method in detecting multiple targets is demonstrated in a wide range of conditions.

ACKNOWLEDGMENT

The authors would like to sincerely thank Mr. Krishna Madan Yelamarty, PhD scholar in the TelWiSe Group at IIT Madras, for the many useful discussions on this work.

REFERENCES

- [1] V. S. Chernyak, *Fundamentals of multisite radar systems: multistatic radars and multistatic radar systems*. Routledge, 2018.
- [2] J. Li and P. Stoica, *MIMO radar signal processing*. John Wiley & Sons, 2008.
- [3] N. H. Nguyen and K. Doğançay, *Signal Processing for Multistatic Radar Systems: Adaptive Waveform Selection, Optimal Geometries and Pseudolinear Tracking Algorithms*. Academic Press, 2019.
- [4] H. Deng and Z. Geng, *Radar networks*. CRC Press, 2020.
- [5] A. M. Haimovich, R. S. Blum, and L. J. Cimini, "MIMO radar with widely separated antennas," *IEEE Signal Process. Mag.*, vol. 25, no. 1, pp. 116–129, 2007.
- [6] H. Li, Z. Wang, J. Liu, and B. Himed, "Moving target detection in distributed MIMO radar on moving platforms," *IEEE J. Sel. Topics Signal Process.*, no. 8, pp. 1524–1535, 2015.
- [7] H. Godrich, A. M. Haimovich, and R. S. Blum, "Target localization accuracy gain in MIMO radar-based systems," *IEEE Trans. Inf. Theory*, vol. 56, no. 6, pp. 2783–2803, 2010.

- [8] A. Noroozi, R. Amiri, M. M. Nayebi, and A. Farina, "Efficient closed-form solution for moving target localization in MIMO radars with minimum number of antennas," *IEEE Trans. Signal Process.*, vol. 68, pp. 2545–2557, 2020.
- [9] S. Sruti, A. A. Kumar, and K. Giridhar, "RCS-based imaging of extended targets for classification in multistatic radar systems," in *Proc. IEEE Radar Conf.* IEEE, 2023, pp. 1–6.
- [10] H. Kuschel, D. Cristallini, and K. E. Olsen, "Tutorial: Passive radar tutorial," *IEEE Aerosp. Electron. Syst. Mag.*, vol. 34, no. 2, pp. 2–19, 2019.
- [11] W. K. Saunders, "CW and FM radar," in *Radar Handbook*, 2nd ed., M. I. Skolnik, Ed. McGraw-Hill, 1990, ch. 14.
- [12] N. Levanon and E. Mozeson, *Radar signals*. John Wiley & Sons, 2004.
- [13] J. J. Benedetto, I. Konstantinidis, and M. Rangaswamy, "The role of the ambiguity function in waveform design and phase coded waveforms," 2008.
- [14] D. Chu, "Polyphase codes with good periodic correlation properties," *IEEE Trans. Inf. Theory*, vol. 18, no. 4, pp. 531–532, 1972.
- [15] J. W. Kang, Y. Whang, B. H. Ko, and K. S. Kim, "Generalized cross-correlation properties of Chu sequences," *IEEE Trans. Inf. Theory*, vol. 58, no. 1, pp. 438–444, 2011.
- [16] A. Noroozi and M. A. Sebt, "Target localization from bistatic range measurements in multi-transmitter multi-receiver passive radar," *IEEE Signal Process. Lett.*, vol. 22, no. 12, pp. 2445–2449, 2015.
- [17] Q. He, R. S. Blum, H. Godrich, and A. M. Haimovich, "Target velocity estimation and antenna placement for mimo radar with widely separated antennas," *IEEE J. Sel. Topics Signal Process.*, vol. 4, no. 1, pp. 79–100, 2010.
- [18] D. Sarwate, "Bounds on crosscorrelation and autocorrelation of sequences," *IEEE Trans. Inf. Theory*, vol. 25, no. 6, pp. 720–724, 1979.
- [19] H.-J. Zepernick and A. Finger, *Pseudo random signal processing: theory and application*. John Wiley & Sons, 2013.
- [20] H. Deng, "Polyphase code design for orthogonal netted radar systems," *IEEE Trans. Signal Process.*, vol. 52, no. 11, pp. 3126–3135, 2004.
- [21] D. Wübben, R. Böhnke, J. Rinas, V. Kühn, and K. D. Kammeyer, "Efficient algorithm for decoding layered space-time codes," *Electronics letters*, vol. 37, no. 22, pp. 1348–1350, 2001.
- [22] S. Vanka, S. Srinivasa, Z. Gong, P. Vizi, K. Stamatidou, and M. Haenggi, "Superposition coding strategies: Design and experimental evaluation," *IEEE Trans. Wireless Commun.*, vol. 11, no. 7, pp. 2628–2639, 2012.
- [23] X.-G. Xia, "Discrete Chirp-Fourier Transform and Its Application to Chirp Rate Estimation," *IEEE Trans. Signal Process.*, vol. 48, no. 11, pp. 3122–3133, 2000.
- [24] A. V. Oppenheim, *Discrete-time signal processing*. Pearson Education India, 1999.
- [25] M. M. U. Gul, X. Ma, and S. Lee, "Timing and frequency synchronization for OFDM downlink transmissions using Zadoff-Chu sequences," *IEEE Trans. Wireless Commun.*, vol. 14, no. 3, pp. 1716–1729, 2014.
- [26] G. Piccinni, G. Avitabile, and G. Coviello, "A novel distance measurement technique for indoor positioning systems based on Zadoff-Chu sequences," in *Proc. Int. New Circuits and Systems Conf. (NEWCAS)*. IEEE, 2017, pp. 337–340.
- [27] K. Lee, J. Kim, J. Jung, and I. Lee, "Zadoff-chu sequence based signature identification for OFDM," *IEEE Trans. Wireless Commun.*, vol. 12, no. 10, pp. 4932–4942, 2013.
- [28] C.-P. Li and W.-C. Huang, "A constructive representation for the fourier dual of the zadoff-chu sequences," *IEEE Trans. Inf. Theory*, vol. 53, no. 11, pp. 4221–4224, 2007.
- [29] J. Li, B. Li, Z. Guo, M. Liu, and Y. Guo, "Multicomponent chirp signal detection based on discrete chirp-Fourier transform," *Wireless Personal Commun.*, vol. 96, pp. 4385–4397, 2017.
- [30] P. Yang, Z. Liu, and W.-L. Jiang, "Parameter estimation of multi-component chirp signals based on discrete chirp Fourier transform and population monte carlo," *Signal, Image and Video Process.*, vol. 9, pp. 1137–1149, 2015.
- [31] X. Huang, S. Tang, L. Zhang, and S. Li, "Ground-based radar detection for high-speed maneuvering target via fast discrete chirp-Fourier transform," *IEEE Access*, vol. 7, pp. 12 097–12 113, 2019.
- [32] C. Wu and B. Chen, "A recognition algorithm of VGPO jamming based on discrete chirp-Fourier transform," *EURASIP J. Adv. Signal Process.*, vol. 2020, no. 1, pp. 1–18, 2020.
- [33] L. B. Almeida, "The fractional fourier transform and time-frequency representations," *IEEE Trans. Signal Process.*, vol. 42, no. 11, pp. 3084–3091, 1994.
- [34] P. Fan and X.-G. Xia, "Two modified discrete chirp fourier transform schemes," *Science in China Series: Inf. Sci.*, vol. 44, pp. 329–341, 2001.
- [35] M. Hua, M. Wang, K. W. Yang, and K. J. Zou, "Analysis of the frequency offset effect on Zadoff-Chu sequence timing performance," *IEEE Trans. Commun.*, vol. 62, no. 11, pp. 4024–4039, 2014.